Leucaena leucocephala and Montmorillonite Co-pyrolysis Biochar: A Study on Physicochemical Properties and Stability

Po-Heng Lin,[a,b] Chun-Han Ko,[a,*] San-Hsien Tu,[b] and Cheng-Jung Lin [b]

Leucaena leucocephala, an invasive toxic tree species, has threatened the survival of native plants in the Hengchun Peninsula, southern Taiwan. Due to the small-to-medium diameter, the utilization and processing of *L. leucocephala* is highly restricted, while its discarding accelerates carbon dioxide emission to the atmosphere. Biochar, produced from the pyrolysis of biomass under an inert atmosphere, is considered an effective carbon sequestration technique with high stability, which is important for long-term carbon storage and soil improvement. *L. leucocephala* biomass and montmorillonite were co-pyrolyzed under inert conditions, aiming to investigate the effects of different pyrolysis temperatures and montmorillonite blending ratios on biochar yield and carbon retention. Results showed improved biochar yield and carbon retention with increasing montmorillonite addition. Thermogravimetric analysis, nuclear magnetic resonance spectroscopy, and Fourier-transform infrared spectroscopy demonstrated enhanced stability of the modified biochars. The production of modified *L. leucocephala* biochar represents a promising technique for carbon dioxide sequestration and biochar stabilization, enabling the development of *L. leucocephala* utilization approaches.

DOI: 10.15376/biores.19.2.3857-3872

Keywords: Leucaena leucocephala; Montmorillonite; Co-pyrolysis; Biochar; Stability

Contact information: a: School of Forestry and Resource Conservation National Taiwan University, Taipei 10617, Taiwan; b: Taiwan Forestry Research Institute, Taipei 100, Taiwan;
**Corresponding authors: chunhank@ntu.edu.tw*

INTRODUCTION

The extensive use of fossil fuels driven by human activities has contributed significantly to the release of carbon dioxide into the atmosphere, exacerbating global warming. The ocean heat content and sea level rise have also increased year by year due to global warming. At the same time, ocean acidification caused by increased carbon dioxide concentrations threatens terrestrial and marine ecosystems. If the current warming rate continues, the 1.5 °C threshold may be reached by 2030-52 (Masson-Delmotte *et al.* 2019). Therefore, reducing greenhouse gas concentrations in the atmosphere has become an important issue internationally in recent years. In this context, carbon dioxide removal (CDR) technologies have been identified by the IPCC as a key approach to reducing atmospheric carbon dioxide levels. Among them, biochar is widely recognized as an effective means of carbon capture and storage (CCS) (Masson-Delmotte *et al.* 2019).

Biochar is a stable carbon-rich solid produced from the thermochemical conversion of biomass in an inert atmosphere. It can be added to soil to improve soil functions, reduce greenhouse gas emissions from biomass and soil, and contribute to carbon storage (IBI 2018). Biochar is considered a potential negative emissions technology (Woolf *et al*. 2010; Smith *et al*. 2020). Its production and incorporation into soil combines CDR with co-benefits for agricultural productivity and soil health (Buss *et al*. 2022). The climate change mitigation applications of biochar build on its highly aromatic C structures that provide high stability, and its developed porous structure and large surface area that impart excellent sorptive capabilities (Wang *et al*. 2016). Studies have also shown biochar's potential as a low-cost sorbent for contaminant immobilization, both organic and inorganic (Houben *et al*. 2013). The amount of biochar used is a key factor, while porosity and surface functional groups determine biochar's effectiveness in metal sorption like Pb and Cr (Yaashikaa *et al*. 2019). Biochar can also improve soil's physicochemical properties, increase soil microbial diversity, and provide more pore space when used as a soil amendment. The increased porosity allows longer residence time for water, air, and nutrients, thereby enhancing microbial growth, survival, and activities, which facilitates plant growth (Yaashikaa *et al*. 2020). In the context of microbial activities in soil, the term "activities" refers to various biological processes carried out by microorganisms. These activities include decomposition, nutrient cycling, nitrogen fixation, and soil structure improvement. These activities are crucial for maintaining soil health and fertility, ultimately benefiting plant growth.

Bruun *et al.* (2014) pointed out that biochar stability in soil is crucial if it is to be used for long-term carbon sequestration and soil quality improvement. Their research found that biochar became mineralized to CO_2 more slowly in soils with higher clay content. Changes in soil clay concentration were observed to impact biochar mineralization rates within the first year of incubation, indicating that biochar experiences physical protection as well as chemical recalcitrance. However, quantitative information regarding the impact of soil properties on biochar stability remains scarce.

Buss *et al*. (2022) summarized that co-pyrolyzing minerals with biomass can increase biochar carbon sequestration potential, optimize nutrient release from the biochar, and enable multifunctional biochar applications. Adding potassium-deficient primary and secondary minerals to biomass during co-pyrolysis may not increase nutrient availability from inherent biomass nutrients, but these minerals could increase stable carbon yields from the biochar, although not all minerals increase biochar stability. In general, clay minerals possess low crystallinity and high reactivity (Scheffer *et al*. 2016). Li tested several clay minerals as additives to straw to examine their catalytic potential during pyrolysis. Adding kaolinite did not increase biochar yield, carbon retention, or carbon stability (Li *et al*. 2014). Liu *et al*. (2020) prepared biochar by co-pyrolyzing biomass (rice straw) and the mineral additive vermiculite at different temperatures to understand the effects and mechanisms of minerals on biochar carbon modification, stabilization, and stability. Their results showed that vermiculite modification increased total mineral content in the biochars, especially iron (Fe), aluminum (Al), magnesium (Mg), and silicon (Si). The formation or enhancement of bonds such as Si-O-C and Fe-O on the biochar surface by vermiculite modification and the promotion of aromatization during carbonization was beneficial for improving biochar stability (Leng and Huang 2018). Lu *et al.* (2020) reacted corn stover with montmorillonite and different iron-bearing minerals through co-pyrolysis to evaluate the impact of iron-modified montmorillonite biochars' surface chemistry and stability. Their results demonstrated that adding iron during pyrolysis facilitated the

formation of organic-metal compounds such as Fe-O-C on the biochar surface. All the iron-modified montmorillonite biochars also exhibited enhanced antioxidant properties. The measured carbon retention index (R_{50}) values of the iron-montmorillonite biochars showed significant increases, suggesting the combination of montmorillonite and iron can effectively improve biochar stability and carbon sequestration potential.

Leucaena leucocephala is among the world's top 100 invasive species, exhibiting allelopathic effects that have heavily encroached on and threatened the survival of native plants in Taiwan's Hengchun Peninsula and Kenting National Park (Chin *et al.* 2007). Lee (2003) used satellite imagery to map *L. leucocephala* distribution in the Hengchun area and found it had invaded 3354 ha of the total 21,363 ha surveyed area, accounting for 15.7% of the area. With most *L. leucocephala* trees being under 10 cm in diameter, utilization is greatly constrained. If discarded in the forest, *L. leucocephala* residue would hamper reforestation efforts and decompose into CO_2, contributing to the increasingly concerning issue of carbon emissions (Hwang 2009). Recent studies have explored various uses for *L. leucocephala* waste, including making it into charcoal or wood ash as biochar activation agents, wood pellets as fuel, and fiberboards after defibration (Lan *et al.* 1991; Peng *et al.* 2010; Chen *et al.* 2010; Hwang *et al.* 2009). Currently, there are no well-established uses for *L. leucocephala*, so most of the wood is either discarded or used as fuel after logging.

This study explored biochar production through co-pyrolysis with clay minerals using the biomass of *L. leucocephala*. The co-pyrolysis aimed to increase carbon retention and stabilize the pyrolyzed carbon in an aromatic form. This could extend the biomaterial's lifetime in soil and delay the release of decomposition CO_2 into the atmosphere, thereby contributing to CDR and overall net zero carbon goals.

The study used thermogravimetric analysis (TGA), the carbon retention index (R_{50}), Fourier transform infrared (FTIR) spectroscopy, and nuclear magnetic resonance (NMR) techniques to verify the increased stability of the produced biochar. It is hoped such efforts could contribute to CCS *via* biochar carbon sequestration and provide a climate change mitigation solution.

EXPERIMENTAL

Materials

The wood material was 3-5-year-old invasive *Leucaena leucocephala* from Taiwan's Hengchun Peninsula. After logging, the bark and wood were manually separated and air-dried.

The wood was crushed using a SY-101 Small Fast Speed Crusher (Shiang Young Machinery, Taiwan) and an RT-08 Pulverizing Machine (Rong Tsong Iron Work, Taiwan). The pulverized wood material was sieved with 80 and 100 mesh screens (Kuang Yang, Taiwan) to obtain wood powder for subsequent experiments. The particles that were considered for the particle size analysis were those that passed through an 80-mesh screen and were retained on a 100-mesh screen. Montmorillonite (Sigma-Aldrich, Germany; CAS 1318-93-0), a common silicate mineral, was used. Phosphoric acid was purchased from Sigma-Aldrich.

Fig. 1. Sample of wooden material (wood), wood mixed with montmorillonite, and montmorillonite

The samples used in this study consisted of wood powder and montmorillonite in the following percentages: 100% *Leucaena* wood powder (LI0), wood powder mixed with 5% montmorillonite (LI5), wood powder mixed with 15% montmorillonite (LI15), wood powder mixed with 20% montmorillonite (LI20), and montmorillonite (M) with phosphoric acid. After crushing, the components were evenly mixed for each sample group.

Sample Characteristic Analysis

The chemical constituents of wood can be categorized into cellulose, hemicellulose, lignin, extractives, and ash. Prior to the analysis of cellulose, hemicellulose, and lignin, extractives were first isolated by alcohol-benzene extraction according to CNS 4713 (2005). The separated cellulose, hemicellulose, and lignin fractions were then quantified individually. Ash, representing the inorganic component, was determined through combustion according to CNS 3084 (2004). The methods mentioned are based on CNS 452 (2013), CNS 4713 (2005), CNS 3084 (2004), CNS 3085 (2004), CNS 14907 (2005), and CNS 12108 (1987). For precise elemental characterization, the materials were analyzed using an Elementar vario EL CUBE elemental analyzer following NIEA R409.21c (2004) to determine the contents of C, H, N, S and O. The methods adopted enabled comprehensive determination of the chemical compositions and constituents of the wood and biochar samples.

Biochar Preparation

The mixtures, organized according to ratio, were placed in ceramic crucibles and evenly blended before loading into a programmable temperature-controlled pyrolysis furnace (N21/M, Nabertherm, Germany). An inert atmosphere was created by continuously supplying 5 L/min of nitrogen gas to purge oxygen from the furnace chamber. Under the inert gas, the furnace was heated at 10 °C/min until reaching pyrolysis temperatures of 350, 375, and 400 °C. The temperature was held at the target for 1 hour to complete pyrolysis. The produced biochars were named according to montmorillonite percentage and pyrolysis temperature as LI0-350, LI5-350, LI15-350, LI20-350, LI0-375, LI5-375, LI15-375, LI20-375, LI0-400, LI5-400, LI15-400, and LI20-400. Each sample was prepared in triplicate.

Comparison of Biochar Properties

Biochar yield and carbon retention percentage are the two fundamental metrics that were used to initially evaluate if the produced biochar can increase carbon retention. The biochar yield was calculated using the formula from Li *et al*. (2014), where biochar yield represents the ratio of the final biochar weight to the initial feedstock weight. Carbon retention was calculated based on the carbon content in the original biomass and the

residual carbon content in the biochar. Thus, carbon retention may be more relevant for estimating carbon sequestration potential. The carbon compositional percentages of the samples were measured using an Elementar vario EL CUBE following the NIEA R409.21c (2004) method mentioned before.

The yield of biochar was calculated as,

$$Yield = \frac{W_{bc} - W_a}{W_b} \times 100 \quad (1)$$

where W_{bc}, W_a, and W_b are the weights of biochar (g) after pyrolysis, ash residual (g), and biomass (g), respectively.

$$Carbon\ retention\ = \frac{W_b \times yield \times C_{bc}}{W_{bc} \times C_b} \times 100 \quad (2)$$

The quantities W_{bc}, W_b, and yield are described above, and C_{bc} and C_b are the total carbon contents of biochar and biomass, respectively.

The specific surface area (m^2/g), representing the total surface area per unit mass of a solid, as well as the porosity, were measured using the Brunauer-Emmett-Teller (BET) analysis to determine the surface area and porosity of the biochars. The Gemini VII surface area and porosity system by Micromeritics, Inc. (USA) was used. Both degassing and analysis were performed with nitrogen gas, and liquid nitrogen was used as the coolant. Particle sizes less than 3.5 mm were used as samples. An appropriate amount of sample was placed in the analysis tube and degassed under vacuum at 150 °C for over 60 minutes. The degassed sample tube was then analyzed by the BET instrument, measuring no less than three points in the relative pressure range of 0.05 to 0.3 *P*/*P*o and taking the average.

Thermogravimetric analysis (TGA) was conducted on the biochars using a Shimazu DTG60 (Japan) with an alumina crucible and lid to examine the thermal decomposition and stability of the main wood components (cellulose, hemicellulose, lignin) after modification. In an inert atmosphere of nitrogen gas, samples were heated from 30 °C to 800 °C at a heating rate of 10 °C/min, with a nitrogen purge of 10 mL/min.

Scanning electron microscopy (SEM, Hitachi S-3000N, Japan) and energy dispersive X-ray (EDS, HORIBA EMAX-ENERGY) analysis were performed to observe the surface morphology and elemental composition of the biochars. After oven-drying at 105 ± 1°C, the samples were mounted on stubs using double-sided tape and sputter coated with gold. The prepared biochar samples were placed in the SEM for observation of the surface microstructure and elemental mapping under vacuum.

Biochar Stability Assessment

Recalcitrance index

The recalcitrance index R_{50} was determined by temperature-programmed oxidation (TPO) of the biochars using a Shimazu DTG60 TGA (Japan) with an alumina crucible and lid. In zero-grade air, samples were heated from 30 °C to 800 °C at 10 °C/min with a purge of 10 mL/min air. The R_{50} values were calculated from the TPO data based on the temperature at which 50% weight loss occurred relative to graphite oxidation at 886 °C, as described by Harvey *et al*. (2012), to quantify the biodegradation resistance of the biochars. T_{50b} represents the temperature at which a sample reaches 50% weight loss during temperature-programmed oxidation:

$$R_{50\,s} = \frac{T_{50\,b}}{T_{50\ graphite}} \quad (3)$$

Attenuated total reflectance Fourier transform infrared spectroscopy (ATR-FTIR)

Changes in the surface functional groups of biochar samples induced by modification can be characterized by attenuated total reflection Fourier transform infrared (ATR-FTIR) spectroscopy. Fourier transform infrared (FTIR) spectra of the samples were obtained using a Varian 2000 (Scimitar Series) FTIR spectrometer (Varian Ltd, USA) equipped with a single-reflection ZnSe ATR accessory (PIKE Inc, USA). The spectra were recorded in attenuated total reflection (ATR) mode with a spectral resolution of 4 cm^{-1} and 64 scans. Prior to analysis, all acquired spectra were corrected for the ATR effect using the ATR correction function in the Varian Resolutions software.

^{13}C solid state nuclear magnetic resonance (NMR)

The ^{13}C CP/MAS NMR spectra were recorded on a Bruker Avance 300 MHz NMR spectrometer (Bruker Spectrospin, Rheinstetten, Germany) equipped with a 4 mm double-resonance MAS probe. The ^{13}C resonance frequency was 75.47 MHz. The MAS rotation frequency was set to 8 kHz using a spinning controller with stability better than 1 Hz. All measurements were performed at room temperature. Chemical shifts were referenced externally to the glycine carbonyl carbon at 176.4 ppm.

Data Analysis

Data analysis was performed using Microsoft Excel 2019. Graphical plots were generated using Origin software.

RESULTS AND DISCUSSION

Physicochemical Characterization of Biochar Samples

As shown in Table 1, the major chemical constituents of the residues of *L. leucocephala*, including total cellulose and hemicellulose, were comparable to the previous findings by Chen *et al.* (2010). The chemical analysis revealed 30.57% lignin, 70.63% holocellulose, 1.88% ash, and 3.84% extractives. The lignin content was analogous to the 29.6 to 33.1% range reported for *L. leucocephala* in earlier literature. The holocellulose percentages obtained were also within the 62.3 to 70.8% literature values. Previous studies showed the extractives to be 0.8 to 4.64%, which is consistent with the observed range in the present work, while the ash content of 1.88% was lower than the range 2.22 to 2.70% documented previously (Chen *et al.* 2010; Al-Mefarrej *et al.* 2011; Amini *et al.* 2019).

Table 1. Chemical Analysis of Wood Materia

Holocellulose (%)	Lignin (%)	Extractives and Others (%)	Ash (%)
70.63	30.57	3.84	1.88

Table 2 shows the changes in physico-chemical properties including biochar yield, carbon retention, and surface area before and after modification with different montmorillonite percentages at various pyrolysis temperatures. The data indicate that as the carbonization temperature increased, the biochar yield gradually decreased. However, biochar yields also showed an increasing trend with montmorillonite addition. Calculating the increase rates revealed that the yield did not linearly correlate with additive amount but rather exhibited a saturating trend.

Table 2. Effects of Montmorillonite Addition Ratio on Biochar Yield, Carbon Retention, Surface Area, and Stability at Different Pyrolysis Temperatures

Sample	Yield (%)	Carbon Retention Ratio (%)	BET (m^2/g)	Biochar Thermal Weight Loss Rate (%)	H/C Atomic Ratio	O/C Atomic Ratio	Recalcitrance Index (R_{50})
LI0-350	40.88	64.25	2.25	62.27	2.04	0.19	52.56
LI5-350	44.92	64.66	2.91	63.65	2.04	0.31	54.62
LI10-350	52.40	68.15	3.76	65.2	2.24	0.41	55.78
LI20-350	67.40	68.41	8.09	66.1	2.81	0.75	57.99
LI0-375	35.34	55.82	2.35	67.33	1.79	0.17	55.94
LI5-375	41.69	60.03	2.99	67.75	1.98	0.28	56.37
LI10-375	48.63	63.32	5.10	70.67	2.11	0.40	56.45
LI20-375	64.78	65.90	10.52	71.12	2.62	0.73	58.09
LI0-400	33.82	55.13	2.77	70.5	1.21	0.16	57.49
LI5-400	39.36	57.29	3.52	70.62	1.31	0.28	58.03
LI10-400	46.58	62.14	5.28	74.63	1.44	0.39	58.05
LI20-400	62.20	64.25	12.60	76.04	1.86	0.71	58.69

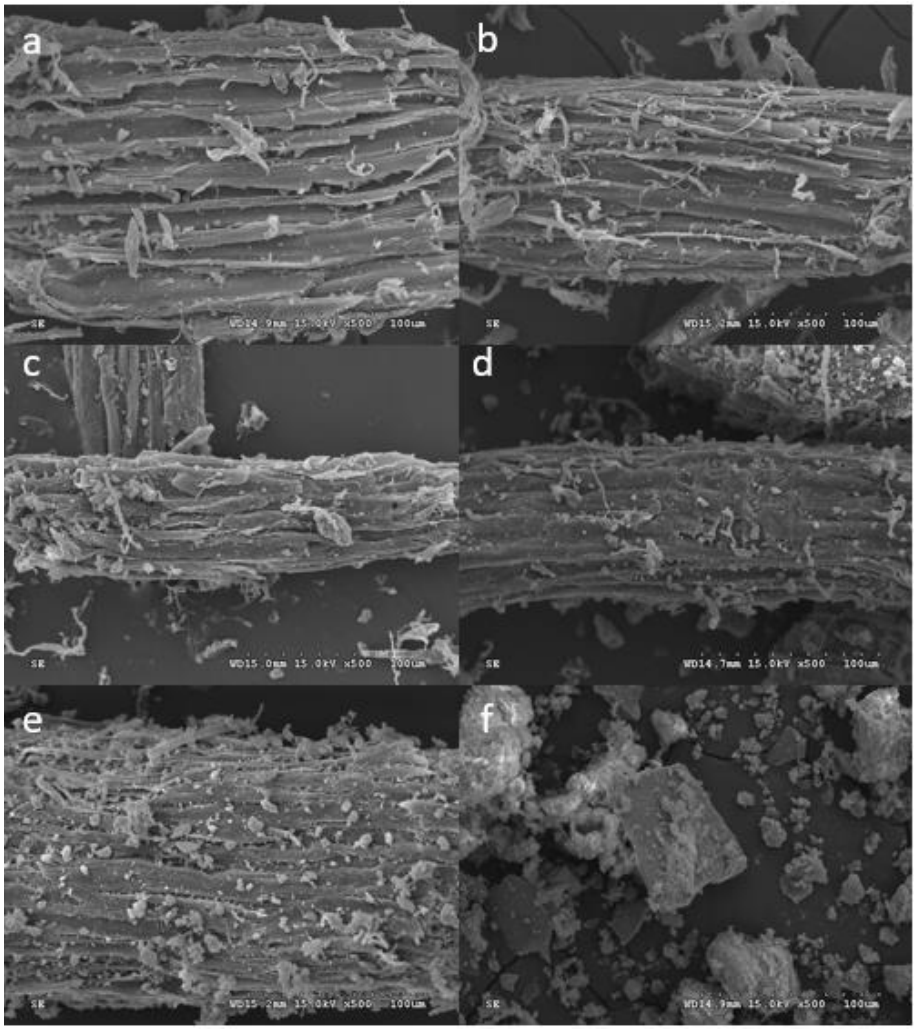

Fig. 2. SEM and EDX analysis of surface morphology of feedstock, unmodified and modified biochars. (a) shows feedstock surface features before pyrolysis. (b) presents biochar surface characteristics after pyrolysis without modification. (c), (d), (e) display biochar surfaces with 5%, 10%, 20% montmorillonite modification. (f) presents montmorillonite surface after pyrolysis.

Montmorillonite modification increased biochar yields, which also rose with increasing pyrolysis temperature. In contrast, carbon retention declined at higher temperatures. At the same temperature, montmorillonite modification improved biochar carbon retention by 3.9 to 16.5%, suggesting that the presence of montmorillonite can effectively enhance biochar's carbon preservation ability and reduce carbon loss during decomposition. This result is similar to that of Lu *et al*. (2020). Additionally, the surface area of unmodified biochar increased from 2.25 to 2.77 as the carbonization temperature increased. At the same pyrolysis temperature, surface area was enhanced to 8.09, 10.52, and 12.60 at 350, 375, and 400 °C, respectively, as montmorillonite percentage rose, indicating montmorillonite modification increased biochar surface area.

To examine the impact of montmorillonite addition on the surface properties of the produced biochars and visualize the morphology of montmorillonite on the biochars, SEM imaging coupled with EDX analysis of elemental distributions in the SEM images was performed. As displayed in Fig. 2(a), the pulverized feedstock surface was where the tissue was torn and crushed by immense external forces, with tiny fragmented tissue scattered on the measured surface and exposed conduits visible due to tissue rupture.

In SEM images Fig. 2(c), (d), (e), many small granules were observed on the surfaces and crevices of biochars with montmorillonite addition, while they were absent on the unmodified biochar surface in Fig. 2(b). EDX analysis (Fig. 2(f)) shows that the montmorillonite contained characteristic Mg, Al, and Si signals. Similarly, the small granules in Fig. 2(c), (d), (e) also exhibited Mg, Al, Si metallic components. This suggests that montmorillonite particles were evenly dispersed on the biochar surface during co-pyrolysis modification. Both the SEM and EDX data analysis indicated that the different montmorillonite percentages led to varying extents of modification by forming mineral-carbon complexes on the biochar surface and pores when thermally decomposing the montmorillonite-treated *Leucaena* wood chips. Further evidence of montmorillonite's impact on *Leucaena* pyrolysis behaviors and biochar properties will be provided by TGA, FTIR, and NMR.

Biochar Stability Assessment

H/C and O/C atomic ratio

The atomic H/C and O/C ratios can characterize the degree of carbon aromatization in biochars, with lower H/C and O/C ratios representing higher aromatization and better stability. As the carbonization temperature increased, the H/C and O/C ratios of the biochars gradually decreased (Table 2), indicating increased aromatic structures. Compared to the more amorphous carbon structures in low-temperature biochars, the aromaticity and stability of high-temperature biochars increased gradually. Studies have shown silicon plays an important role in carbon ordering and compositional structure in rice straw biochars (Guo and Chen 2014). However, adding montmorillonite increased the H/C and O/C ratios of the biochars, likely because the montmorillonite composition itself contains H and O, which raises the H/C and O/C ratios (Han *et al*. 2018). Research has suggested that silicon may combine with carbon to form dense protective structures, thereby enhancing biochar stability.

Thermogravimetric analysis

Figure 3 shows the thermogravimetric (TG) and DTG analyses of *Leucaena* wood powder, montmorillonite, and biochars from co-pyrolysis of wood powder with 0, 5, 10, and 20% montmorillonite. Figure 3(a) shows TG curves of wood powder and

montmorillonite. Figure 3(b) displays biochar TG curves with different montmorillonite percentages. Figures 3(c) and (d) present DTG curves corresponding to Figs. 3(a) and (b).

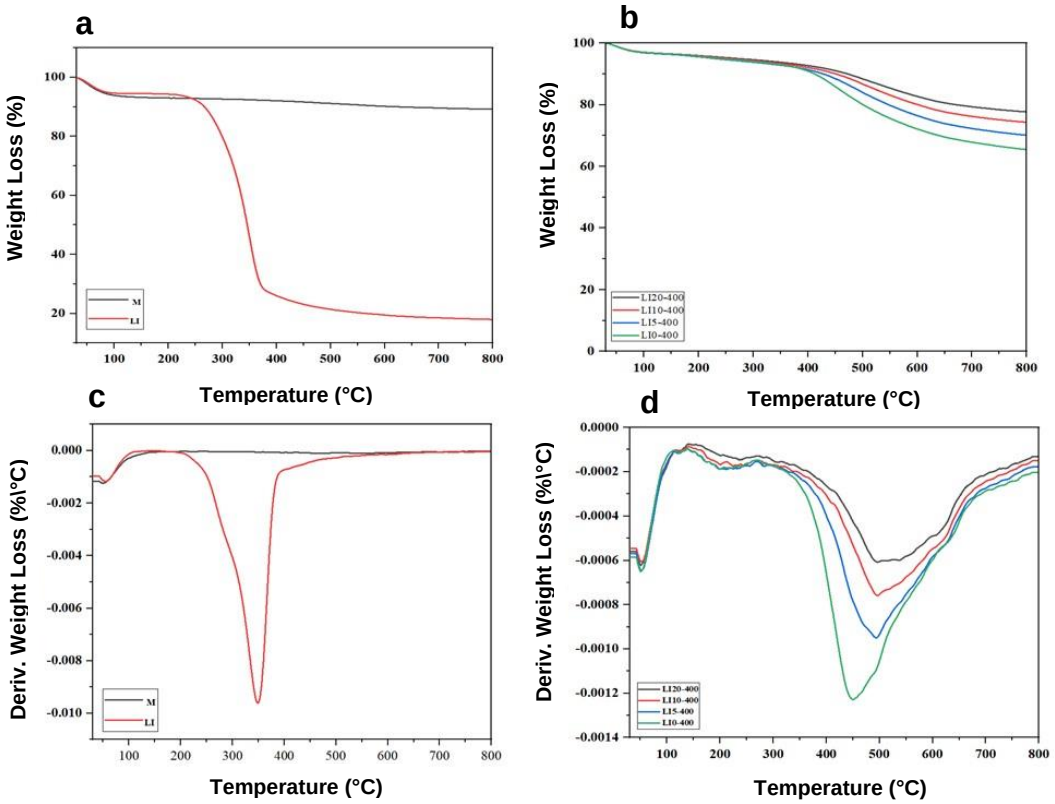

Fig. 3. Thermogravimetric (TG) and DTG analysis of *Leucaena* wood powder, montmorillonite, and biochars from co-pyrolysis of wood powder with 0, 5, 10, 20% montmorillonite

Thermogravimetric analysis utilizes precise temperature programming to induce sample weight losses as temperature increases, revealing thermal decomposition behaviors. The TG curve in Fig. 3(a) shows that the *Leucaena* wood powder exhibited three decomposition stages: (1) RT-150 °C with moisture and some volatiles lost, (2) 150 to 500 °C with maximum decomposition and ~70% weight loss mainly from cellulose and hemicellulose, and (3) 500 to 800 °C with final decomposition primarily of lignin. The residual percentage at 800 °C represents the remaining solid. This aligns with Loaiza *et al*. (2017), who reported that *Leucaena* thermally decomposes based on its lignocellulosic components. Montmorillonite is an inorganic clay mineral with magnesium aluminum silicate octahedral layers. Figure 3(c) shows it exhibits minimal decomposition except for stage 1, consistent with Olad and Azhar (2014).

TGA can assess biochar thermal stability. Figure 3(b) displays TG and DTG curves of biochars with different montmorillonite percentages, with decreased thermal weight losses as an additive percentage and pyrolysis temperature increased. Figures 3(c) and (d) show that the original wood powder has a maximum decomposition rate temperature (TP) of 350 °C. After pyrolysis, the biochar TP value was increased to 449 °C, and TP rose from 493 to 518 °C as montmorillonite percentage grew, with similar trends at other temperatures. The shifting of TP to higher values indicates enhanced thermal stability of the modified biochars. The improved montmorillonite-biochars had 18.7% lower weight loss, confirming increased thermal stability from montmorillonite modification. This may

be because montmorillonite evenly distributes on the biomass and first absorbs heat during decomposition, thermally protecting the biochar through barrier effects (Fajnor and Jesenák 1996).

Further thermogravimetric analysis was performed to compare the thermal weight losses of *Leucaena* wood powder and montmorillonite with their biochars produced at different temperature regions. According to Yang *et al*. (2007), the weight loss percentage from room temperature to 150 °C represents sample moisture content; 220 to 315 °C represents hemicellulose content; 315 to 400 °C represents cellulose content; and 400 to 800 °C represents lignin content. The remaining weight percentage is considered as residue. For the LI sample, the moisture content was 5.53%; hemicellulose pyrolysis temperature region weight loss was 21.1%; cellulose pyrolysis temperature region weight loss was 46.8%; lignin pyrolysis temperature region weight loss was 8.1%; and residue was 18.0%.

The results showed that after carbonization treatment, the moisture content decreased, and the weight loss percentages in the representative pyrolysis temperature regions for cellulose, hemicellulose, and lignin all significantly declined compared to the original *Leucaena* wood powder, regardless of montmorillonite addition. However, the residue percentage increased markedly with more montmorillonite blending (from 18.0 to the range 65 to 77%). This indicates the montmorillonite-modified biochars require higher temperatures for thermal decomposition, thus enhancing their thermal stability.

Recalcitrance index (R_{50})

The recalcitrance index (R_{50}) evaluates biochar quality for carbon sequestration by comparing its thermal stability to that of graphite (Harvey *et al*. 2012). Biochars are classified based on their R_{50} values: $R_{50} > 0.7$ indicates highly recalcitrant biochar, similar to graphite. $R_{50} \leq 0.5$ indicates easily degradable biochar, similar to uncarbonized biomass. Intermediate R_{50} values signify intermediate recalcitrance between the above extremes. The R_{50} of *Leucaena* wood powder was 0.3. After pyrolysis at 400 K, the resulting biochar had an R_{50} of 0.57. As the montmorillonite percentage increased, the R_{50} also exhibited an increasing trend, reaching a maximum of 58.7 at 20% addition.

These results demonstrate that adding montmorillonite enhances the stability and antioxidant properties of the biochar, improving its carbon sequestration potential. The increase in R_{50} with montmorillonite addition aligns with findings by Lu *et al*. (2020), who found that minerals can increase biochar recalcitrance.

^{13}C solid state NMR spectrum

Figure 4 shows the nuclear magnetic resonance (NMR) spectra of *Leucaena* biochars and montmorillonite-modified biochars. The NMR spectra indicate that the main carbon functional groups in the uncarbonized *Leucaena* wood powder are alkyl C (90-0 ppm) while aromatic C (165 to 110 ppm) has relatively lower content. After pyrolysis, the biochar NMR spectra show that aromatic C (165 to 110 ppm) became the predominant functional group, contributing to high aromaticity. As the carbonization temperature increased, aromatic C increased while alkyl C decreased in the biochars. This aligns with the findings of Qi *et al*. (2021), who reported that higher pyrolysis temperatures result in greater biochar aromatization. The carbonization temperatures of 350 to 400 °C used in this study are expected to induce dehydration, thermal decomposition, and carbonization of the large biomolecules, with molecular weight reduction and aromatic ring formation during pyrolysis. Condensed aromatic ring stacking continues developing with further temperature increases (Li *et al*. 2021).

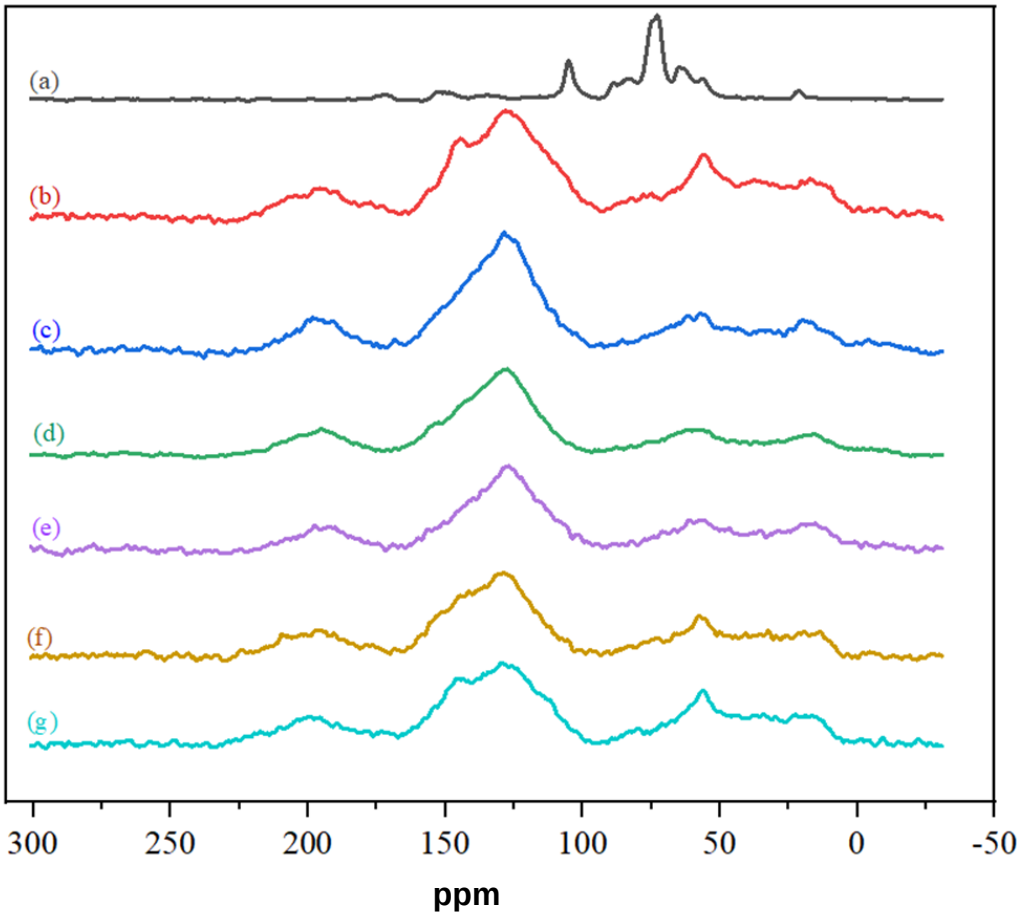

Fig. 4. NMR spectra of modified and unmodified biochar. (a) *Leucaena leucocephala* powder、(b) LI0-350, (c) LI0-375, (d) LI0-400, (e) LI5-400, (f) LI10-400, and (g) LI20-400)

Fan *et al*. (2020) stated that co-pyrolysis with montmorillonite provides Al, Fe, Mg, Si, and other minerals that increase the aromatization degree of biochars during carbonization, *i.e.* the conversion rate of C from alkyl and carbonyl C to aromatic C. This enhances biochar stability. Guo *et al*. (2019) also reported that C-O-Fe, C-O-Mg, C-O-Si, and other metal-oxygen-carbon bonds in montmorillonite-modified biochars have ^{13}C NMR chemical shifts of 90 to 50 ppm. The increase at 60 to 50 ppm observed in the NMR spectra with montmorillonite addition is attributed to such metal-oxygen-carbon bonds. FTIR spectroscopy further confirmed changes in the surface functional groups of modified and unmodified biochars.

FTIR spectrum

Figure 5 shows the FTIR spectra of *Leucaena* biochars before and after montmorillonite modification, providing further evidence of changes in surface functional groups of the unmodified and modified biochars. The absorbance peak at 3400 cm^{-1} corresponds to O-H stretching vibration. As shown in Fig. 5(a), the uncarbonized wood powder exhibited the strongest O-H absorbance, since it did not undergo pyrolysis. O-H absorbance progressively decreased with higher montmorillonite percentages. Figure 5(b) shows O-H absorption also declined with increasing carbonization temperature, aligning with Liu *et al*. (2020) that pyrolysis decreases the number of hydroxyl groups.

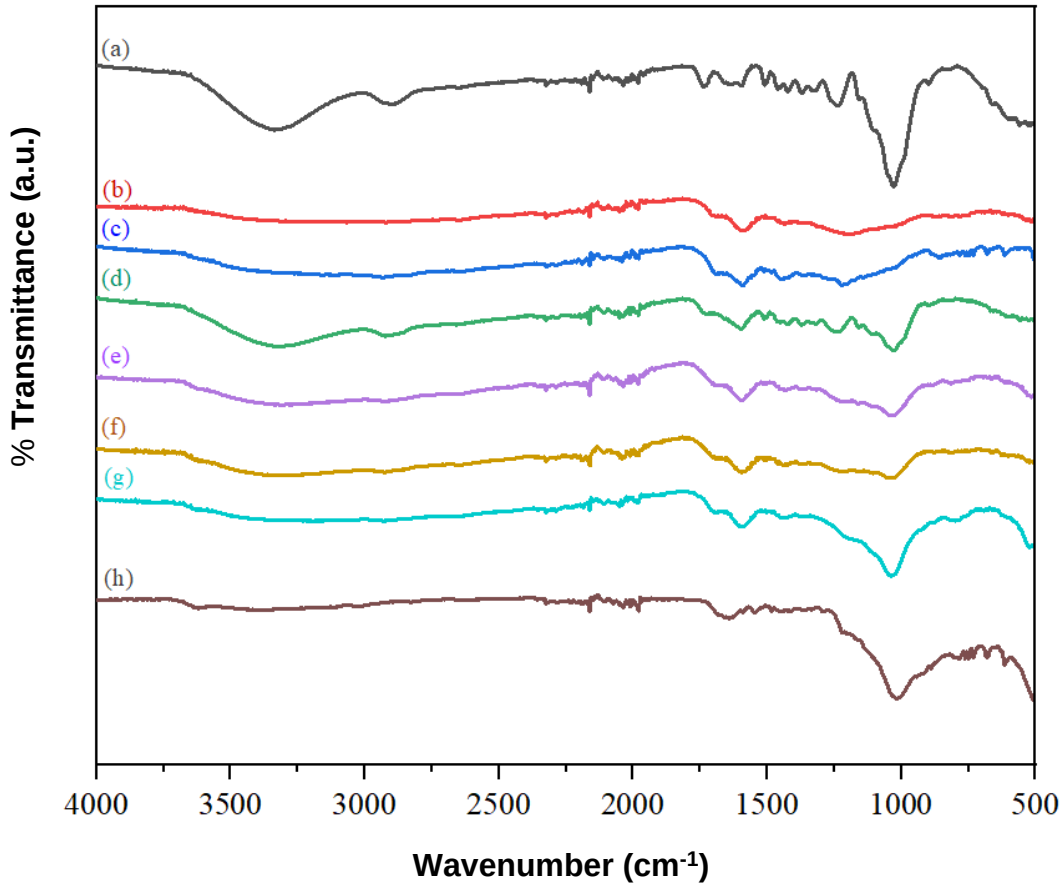

Fig. 5. FTIR spectra of modified and unmodified biochar. (a) *Leucaena leucocephala* powder, (b) LI0-400, (c) LI0-375, (d) LI0-350, (e) LI5-400, (f) LI10-400, (g) LI20-400, and (h) Montmorillonite

The peak at 2950 cm^{-1} represents C-H stretching vibration. The spectra demonstrate this absorbance diminished and eventually disappeared as both pyrolysis temperature and montmorillonite percentage rose. The characteristic peak at 1710 cm^{-1} corresponds to C=O stretching vibration. The results display a slight increase in this absorption with higher temperature and additive levels, which can be attributed to dehydration reactions between functional groups during carbonization according to Liu *et al*. (2020).

The attenuation of C-O-C stretching vibration (1100 cm^{-1}) corresponding to ether groups, replaced by absorption of Si-O-C or Si-O-Si groups (1100 to 1000 cm^{-1}), indicates the modified biochars have more stable mineral-organic complexes on the surface (Guo and Chen 2014).

As described by Chen *et al*. (2022), the Mg-O vibration absorbance at 400 to 600 cm^{-1} became more intense with increasing montmorillonite percentage due to the Mg content of montmorillonite. The growth of this peak signifies the likely presence of magnesium complexes and oxides on the modified biochar surface, consistent with the SEM imaging and EDX analysis.

CONCLUSIONS

1. This study revealed that the incorporation of montmorillonite as a modifier resulted in an enhanced biochar yield. The magnitude of this effect exhibited a positive correlation with increasing pyrolysis temperature. Under the same pyrolysis temperature, montmorillonite modification enhanced the carbon retention of biochar by 3.9 to 16.5%. This implies that montmorillonite presence can effectively improve the carbon preservation capacity of biochar and mitigate carbon loss during pyrolysis.
2. Regarding biochar properties, the specific surface area increased up to 12.6 m^2/g with more montmorillonite addition under the same pyrolysis temperature. This suggests montmorillonite modification may enlarge the specific surface area of biochar, which could benefit the modification of soil properties. Scanning electron microscopy with energy dispersive X-ray (SEM-EDX) data indicated that montmorillonite-carbon complexes had formed on biochar surfaces and pores after co-pyrolysis of and different *L. leucocephala* blending ratios of montmorillonite.
3. Thermogravimetric analysis (TGA) revealed shifts in the maximum mass loss temperature toward higher temperature regions. This demonstrates the enhanced thermal stability of the modified biochars by montmorillonite incorporation. The reduced mass loss by 18.7% in the modified montmorillonite-biochars further implies that montmorillonite modification can reinforce the thermal stability of biochar.
4. The investigation of biochar stability through the recalcitrance index (R_{50}) and NMR and FTIR spectroscopy showed increased R_{50} values with more montmorillonite loading, reaching the maximum of 0.587 at 20% loading under 400 K pyrolysis. This suggests montmorillonite augmentation may strengthen the stability and oxidation resistance of biochar, improving carbon sequestration. Also, NMR and FTIR spectra exhibited an increase of aromaticity in biochars, enhancing stability after modification.

ACKNOWLEDGMENTS

This research was supported by grants from Taiwan Forestry Research Institute, the Ministry of Agriculture, Taiwan.

REFERENCES CITED

Al-Mefarrej, H. A., Abdel-Aal, M. A., Nasser, R. A., and Shetta, N. D. (2011). "Impact of initial tree spacing and stem height level on chemical composition of *Leucaena Leucocephala* tress grown in Riyadh region," *World Appl. Sci. J.* 12(7).

Amini, E., Safdari, M. S., DeYoung, J. T., and Weise, D. R. (2019). "Characterization of pyrolysis products from slow pyrolysis of live and dead vegetation native to the southern United States," *Fuel* 235(1), 1475-1491. DOI: 10.1016/j.fuel.2018.08.112

Bruun, S., Clauson-Kaas, S., Bobuľská, L., and Thomsen, I. K. (2014). "Carbon dioxide emissions from biochar in soil: Role of clay, microorganisms and carbonates," *European Journal of Soil Science* 65(1), 52-59. DOI: 10.1111/ejss.12073

Buss, W., Wurzer, C., Manning, D. A., Rohling, E. J., Borevitz, J., and Mašek, O. (2022).

"Mineral-enriched biochar delivers enhanced nutrient recovery and carbon dioxide removal," *Communications Earth and Environment* 3(1), 67. DOI: 10.1038/s43247-022-00394-w

Chen, T. T., Huang, J. C., Li, R. X., Huang, C. Y., Lin, Y. C., Juan, S. W., and Soong, H. D. (2010). "The rudimentary investigation on manufacturing and properties of pelletized fuels from white popinac (*Leucaena leucocephala*)," *Forest Products Industries* 29(2), 109-120.

Chen, W., Feng, J., Liu, S., Zhang, J., Cai, Y., Lv, Z., Fang, M., and Tan, X. (2022). "A green and economical MgO/biochar composite for the removal of U (VI) from aqueous solutions," *Chemical Engineering Research and Design* 180, 391-401. DOI: 10.1016/j.cherd.2022.02.031

Chin, C. C., Wei, C. H., and Chen, C. T. (2007). "Study on the Invasion of *Leucaena leucocephala* in Kenting National Park. *Hwa Kang Journal of Agriculture* (20), P41-51. DOI: 10.29985/HKJA.200712.0003

CNS 452 (2013). "Wood – Determination of moisture content for physical and mechanical tests," Chinese National Standards, Taipei, Taiwan.

CNS4713 (2005). "Method of test for ethanol-toluene extractives in wood," Chinese National Standards, Taipei, Taiwan.

CNS3084 (2004). "Method of test for ash in wood," Chinese National Standards, Taipei, Taiwan.

CNS 3085 (2004). "Method of test for holocellulose in wood," Chinese National Standards, Taipei, Taiwan.

CNS 14907 (2005). "Method of test for acid-insoluble lignin in wood," Chinese National Standards, Taipei, Taiwan.

CNS12108 (1987). "Method of test for acid-soluble lignin in wood and pulp," Chinese National Standards, Taipei, Taiwan.

Fajnor, V. Š., and Jesenák, K. (1996). "Differential thermal analysis of montmorillonite," *Journal of Thermal Analysis* 46, 489-493. DOI: 10.1007/BF02135026

Fan, J., Li, Y., Yu, H., Li, Y., Yuan, Q., Xiao, H., Li, F., and Pan, B. (2020). "Using sewage sludge with high ash content for biochar production and Cu (II) sorption," *Science of the Total Environment* 713, article 136663. DOI: 10.1016/j.scitotenv.2020.136663

Guo, J., and Chen, B. (2014). "Insights on the molecular mechanism for the recalcitrance of biochars: Interactive effects of carbon and silicon components," *Environmental Science and Technology* 48(16), 9103-9112. DOI: 10.1021/es405647e

Guo, W., Lu, S., Shi, J., and Zhao, X. (2019). "Effect of corn straw biochar application to sediments on the adsorption of 17α-ethinyl estradiol and perfluorooctane sulfonate at sediment-water interface," *Ecotoxicology and Environmental Safety* 174, 363-369. DOI: 10.1016/j.ecoenv.2019.01.128

Han, L., Ro, K. S., Wang, Y., Sun, K., Sun, H., Libra, J. A., and Xing, B. (2018). "Oxidation resistance of biochars as a function of feedstock and pyrolysis condition," *Science of the Total Environment* 616, 335-344. DOI: 10.1016/j.scitotenv.2017.11.014

Harvey, O. R., Kuo, L. J., Zimmerman, A. R., Louchouarn, P., Amonette, J. E., and Herbert, B. E. (2012). "An index-based approach to assessing recalcitrance and soil carbon sequestration potential of engineered black carbons (biochars)," *Environmental Science and Technology* 46(3), 1415-1421. DOI: 10.1021/es2040398

Houben, D., Evrard, L., and Sonnet, P. (2013). "Mobility, bioavailability and pH-

dependent leaching of cadmium, zinc and lead in a contaminated soil amended with biochar. *Chemosphere* 92(11), 1450-1457. DOI: 10.1016/j.chemosphere.2013.03.055

Hwang, G. S. (2009). "Assessing the carbon retention benefits of firing charcoal from *Leucaena leucocephala* waste wood," *TFRI Extension Series* 16(5), 33-35. DOI: 10.29953/FRN.200910.0007

IBI (2018). "Frequently asked questions about biochar: What is biochar?," International Biochar Initiative (IBI), (https://biochar–international.org/faqs).

Lan, H. F., and Huang, Y. F. (1991). "Manufacturing of medium density fiberboard(II) schefflera trees, formosan alder, India-charcoal trema and giant *Leucaena* as raw material for fiberboard manufacture," *Forest Products Industries* 10(1), 35-49. DOI: 10.6561/FPI.1991.10(1).3

Lee, J. T. (2003). "Study on the spread and invasion of *Leucaena leucocephala* in Hengchung Area," *Department of Forestry, National Pingtung University of Science and Technology, Pingtung, Taiwan (in Chinese)*.

Leng, L., and Huang, H. (2018). "An overview of the effect of pyrolysis process parameters on biochar stability," *Bioresource Technology* 270, 627-642. DOI: 10.1016/j.biortech.2018.09.030

Li, C., Zhang, C., Zhang, L., Gholizadeh, M., and Hu, X. (2021). "Biochar catalyzing polymerization of the volatiles from pyrolysis of poplar wood," *International Journal of Energy Research* 45(9), 13936-13951. DOI: 10.1002/er.6733

Li, F., Cao, X., Zhao, L., Wang, J., and Ding, Z. (2014). "Effects of mineral additives on biochar formation: Carbon retention, stability, and properties," *Environmental Science and Technology* 48(19), 11211-11217. DOI: 10.1021/es501885n

Liu, Y., Gao, C., Wang, Y., He, L., Lu, H., and Yang, S. (2020). "Vermiculite modification increases carbon retention and stability of rice straw biochar at different carbonization temperatures," *Journal of Cleaner Production* 254, article 120111. DOI: 10.1016/j.jclepro.2020.120111

Loaiza, J. M., López, F., García, M. T., García, J. C., and Díaz, M. J. (2017). "Biomass valorization by using a sequence of acid hydrolysis and pyrolysis processes. Application to *Leucaena leucocephala*," *Fuel* 203, 393-402. DOI: 0010.1016/j.fuel.2017.04.135

Lu, J., Yang, Y., Liu, P., Li, Y., Huang, F., Zeng, L., and Hou, B. (2020). "Iron-montmorillonite treated corn straw biochar: Interfacial chemical behavior and stability," *Science of the Total Environment* 708, article 134773. DOI: 10.1016/j.scitotenv.2019.134773

Masson-Delmotte, V., Zhai, P., Pörtner, H. O., Roberts, D., Skea, J., Shukla, P. R., and Waterfield, T. (2019). "Global warming of 1.5 °C," *An IPCC Special Report on the Impacts of Global Warming of*, 1, 93-174.

NIEA R409.21C (2004). "Content determination method of carbon, hydrogen, sulfur, oxide and nitrogen in the waste-elemental analyzer," Environmental Protection Administration, Taipei, Taiwan.

Olad, A., and Azhar, F. F. (2014). "Eco-friendly biopolymer/clay/conducting polymer nanocomposite: characterization and its application in reactive dye removal," *Fibers and Polymers* 15, 1321-1329. DOI: 10.1007/s12221-014-1321-6

Peng, C. W., Wang, Y. N., Shiah, T. C., Chung, M. J., and Lin, H. C. (2010). "Investigation on white popinac (*Leucaena leucocephala*) ash as a natural activating agent for activated carbon preparation," *Journal of the Experimental Forest of National Taiwan University* 24(4), P247-260. DOI:

10.6542/EFNTU.201010_24(4).0004
Qi, Q., Sun, C., Cristhian, C., Zhang, T., Zhang, J., Tian, H., He, Y., and Tong, Y. W. (2021). "Enhancement of methanogenic performance by gasification biochar on anaerobic digestion," *Bioresource Technology* 330, article 124993. DOI: 10.1016/j.biortech.2021.124993
Scheffer, F., Schachtschabel, P., and Blume, H. P. (2016). *Scheffer/Schachtschabel Soil Science*. Springer. DOI: 10.1007/978-3-642-30942-7_8
Smith, P., Calvin, K., Nkem, J., Campbell, D., Cherubini, F., Grassi, G., Korotkov, V., Hoang, A. L., Lwasa, S., McElwee, P., *et al.* (2020). "Which practices co-deliver food security, climate change mitigation and adaptation, and combat land degradation and desertification?," *Global Change Biology* 26(3), 1532-1575. DOI: 10.1111/gcb.14878
Wang, Y. Y., Lu, H. H., Liu, Y. X., and Yang, S. M. (2016). "Ammonium citrate-modified biochar: An adsorbent for La (III) ions from aqueous solution," *Colloids and Surfaces A: Physicochemical and Engineering Aspects* 509, 550-563. DOI: 10.1016/j.colsurfa.2016.09.060
Woolf, D., Amonette, J. E., Street-Perrott, F. A., Lehmann, J., and Joseph, S. (2010). "Sustainable biochar to mitigate global climate change," *Nature communications* 1(1), 56. DOI: 10.1038/ncomms1053
Yaashikaa, P. R., Kumar, P. S., Babu, V. M., Durga, R. K., Manivasagan, V., Saranya, K., and Saravanan, A. (2019). "Modelling on the removal of Cr (VI) ions from aquatic system using mixed biosorbent (*Pseudomonas stutzeri* and acid treated Banyan tree bark)," *Journal of Molecular Liquids* 276, 362-370. DOI: 10.1016/j.molliq.2018.12.004
Yaashikaa, P. R., Kumar, P. S., Varjani, S., and Saravanan, A. (2020). "A critical review on the biochar production techniques, characterization, stability and applications for circular bioeconomy," *Biotechnology Reports* 28, article e00570. DOI: 10.1016/j.btre.2020.e00570
Yang, H., Yan, R., Chen, H., Lee, D. H., and Zheng, C. (2007). "Characteristics of hemicellulose, cellulose, and lignin pyrolysis," *Fuel* 86(12-13), 1781-1788. DOI: 10.1016/j.fuel.2006.12.013

Article submitted: November 27, 2023; Peer review completed: March 9, 2024; Revised version received: April 11, 2024; Accepted: April 13, 2024; Published: April 30, 2024.
DOI: 10.15376/biores.19.2.3857-3872